

Ferromagnetism and crystal fields in YbInNi_4

J. L. Sarrao

*National High Magnetic Field Laboratory, Florida State University, Tallahassee, Florida 32306
and MST Division, Los Alamos National Laboratory, Los Alamos, New Mexico 87545*

R. Modler, R. Movshovich, A. H. Lacerda, D. Hristova, A. L. Cornelius, M. F. Hundley, and J. D. Thompson
MST Division, Los Alamos National Laboratory, Los Alamos, New Mexico 87545

C. L. Benton, C. D. Immer, M. E. Torelli, G. B. Martins, and Z. Fisk
National High Magnetic Field Laboratory, Florida State University, Tallahassee, Florida 32306

S. B. Oseroff

Department of Physics, San Diego State University, San Diego, California 92182

(Received 25 September 1997)

We present transport and thermodynamic measurements as a function of temperature (0.1–300 K), pressure (1 bar–16 kbars), and magnetic field (0–600 kOe) on YbInNi_4 . Ferromagnetism arises near 3 K out of a state with enhanced electronic specific-heat coefficient. Resistivity, specific-heat, and magnetization measurements imply that the ground state of YbInNi_4 is a crystal-field doublet, whereas earlier neutron-scattering results suggest a ground-state quartet. We also compare YbInNi_4 to YbInCu_4 and intermediate alloys. [S0163-1829(98)00613-4]

I. INTRODUCTION

Because of the near degeneracy of Yb's f^{13} and f^{14} configurations, many Yb compounds display intermediate-valence or heavy fermion behavior.¹ In this sense, Yb may be thought of as the “ f -hole” analog of Ce, whose f^0 and f^1 configurations give rise to similar phenomena. The competition between localized and itinerant f -electron behavior gives rise to a wealth of ground states in intermetallic compounds that depend significantly on rather subtle differences in lattice constant and ligand ions.² As such, the systematic study of the evolution of physical properties with chemical composition has been a fruitful area of research in the study of f -electron materials.

YbXM_4 compounds (where X is a semimetal or late transition metal and M is a transition metal) have attracted attention because of the wide variety of ground states displayed in this isostructural series. In particular, YbInCu_4 exhibits an isostructural valence transition,^{3–10} YbAgCu_4 displays heavy fermion behavior with no magnetic order to the lowest temperatures measured,^{11–13} and YbPdCu_4 and YbAuCu_4 order magnetically below 1 K.^{11,13–15} The Ni variants of these compounds are relatively unstudied.^{16–18}

Here, we present the results of a detailed study of the physical properties of single-crystal YbInNi_4 . YbInNi_4 orders ferromagnetically at low temperature, a relatively uncommon ground state for trivalent Yb compounds—only a few examples of such behavior are known: the dense Kondo compound YbNiSn ,^{19–21} $\text{Yb}_2\text{Ni}_{17}$, in which the Ni sublattice also orders ferromagnetically,^{22,23} and YbPt_2 .²⁴ However, as discussed below, crystal-field effects are dominant in YbInNi_4 , making it more analogous to the antiferromagnetic compound YbBe_{13} (Refs. 25–28) than to YbNiSn .

II. EXPERIMENTAL DETAILS

We have grown single crystals of YbInNi_4 using an In-Ni flux in a manner similar to that employed in Ref. 4. YbInNi_4 crystallizes in the cubic AuBe_5 ($C15b$) structure with a lattice constant of 6.98 Å, as determined by powder x-ray diffraction (see also Refs. 16–18). The Yb and In ions sit on distinct face-centered-cubic sublattices displaced by $(1/4, 1/4, 1/4)$ along the body diagonal and are surrounded by space-filling Ni tetrahedra. The single crystals have a well-faceted, tetrahedral morphology with typical dimension 3–5 mm. Measured physical properties are quantitatively reproducible from batch to batch and are insensitive to the precise composition and temperature profiles used in the flux growths.

A variety of experimental techniques have been employed to span the range of parameter space for which we report data. A superconducting quantum interference device magnetometer was used to measure the temperature-dependent magnetic susceptibility and isothermal magnetization, as well as to provide an absolute calibration to high-field magnetization measurements. Electrical resistivity measurements as a function of pressure and temperature were performed in a He³ cryostat using a Be/Cu clamp-type pressure cell with flourinert as the pressure transmitting medium. For temperatures above 1.5 K, a thermal relaxation technique was used to determine specific heat,²⁹ while for temperatures below 2 K, a quasiadiabatic method was used. The agreement between these techniques in the range of temperature overlap is excellent. Magnetoresistance measurements were performed in a 200 kOe superconducting magnet with the magnetic field applied perpendicular to the measurement current, and high-field magnetization measurements were performed in a 600 kOe pulsed magnet using a mutual inductance technique. Both high-field magnets are located at the National High Magnetic Field Laboratory—Los Alamos Pulsed Field Facility.

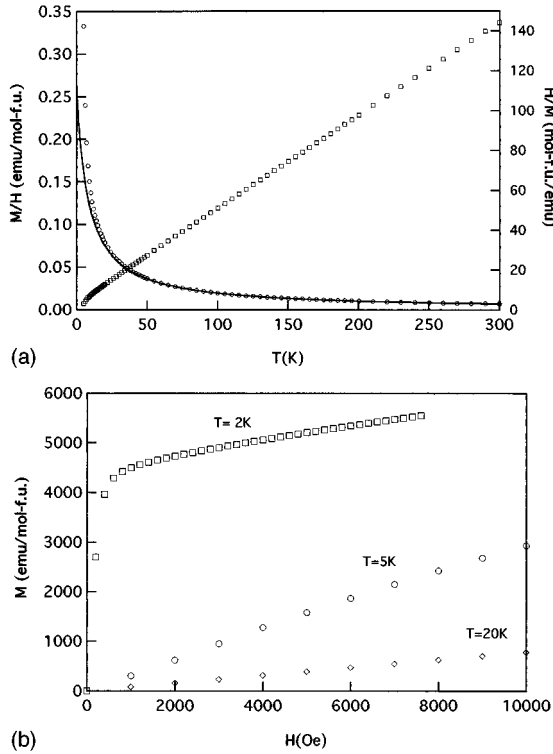


FIG. 1. (a) Magnetic susceptibility (circles) and inverse magnetic susceptibility (squares) for YbInNi_4 . The solid line is a Curie-Weiss fit to the data which gives $\mu_{\text{eff}}=4.11\mu_B$ and $\theta=8.2$ K. (b) Isothermal magnetization as a function of field at various temperatures for YbInNi_4 .

III. RESULTS

In Fig. 1(a) we show the magnetic susceptibility of YbInNi_4 as a function of temperature. The high-temperature data are well-fit by a Curie-Weiss law with effective moment $4.11\mu_B$, nearly the full free-ion Yb value, and an antiferromagnetic Weiss temperature of 8.2 K. The deviation from Curie-Weiss behavior at low temperature is suggestive of crystal-field effects, a suggestion to be discussed in detail below, as well as the onset of short-range ferromagnetic correlations. Isothermal magnetization data in Fig. 1(b) indicate that YbInNi_4 orders ferromagnetically (consistent with previous observations¹⁶) at low temperature with nearly $1\mu_B$ of ordered moment. Note, however, that by 1 T, the magnetization is only weakly saturated. If one estimates the susceptibility at 2 K from $\Delta M/\Delta H$ in this region, one finds a susceptibility that is $\sim 50\%$ of that expected from the high- T Curie-Weiss fit. This susceptibility is presumably due to a change in the population of excited crystal-field states with increasing magnetic field.

The electrical resistivity as a function of temperature and pressure is shown in Fig. 2. YbInNi_4 is a relatively good metal with a residual resistivity of only $10\mu\Omega$ cm. Two principal features are apparent in the 1-bar temperature-dependent resistivity: a shoulderlike feature near 20 K, suggestive of either the onset of Kondo coherence or the influence of crystal-electric fields, and a sharp drop at 3 K, consistent with the onset of magnetic order. The application of 16 kbars of hydrostatic pressure has no effect on either the magnetic ordering temperature or the position or magnitude

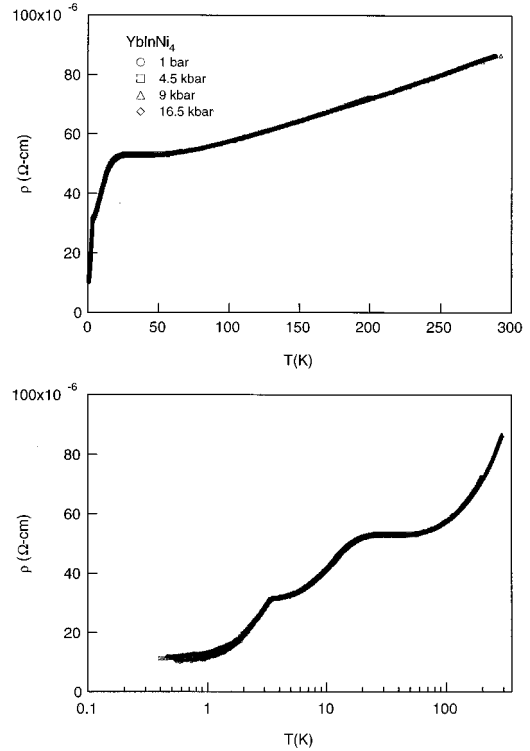


FIG. 2. Electrical resistivity as a function of temperature for YbInNi_4 (upper panel: linear T scale; lower panel: logarithmic T scale). The data at fixed pressures of 1 bar, 4.5, 9, and 16.5 kbars are indistinguishable.

of the 20-K feature. This argues strongly for a crystal-field-induced drop in resistivity.³⁰ Kondo coherence effects usually depend strongly on pressure due to the pressure dependence of the exchange coupling constant J .³¹ For the case of crystal-field effects, Cornut and Coqblin³⁰ have shown that a drop in resistivity generally occurs at 0.7Δ , where Δ is the energy splitting between the ground state and the first excited crystal-field state. For YbInNi_4 this would imply a first excited state approximately 30 K above the ground state.

The temperature-dependent specific heat of YbInNi_4 is depicted in Fig. 3. Below 20 K the zero-field data are domi-

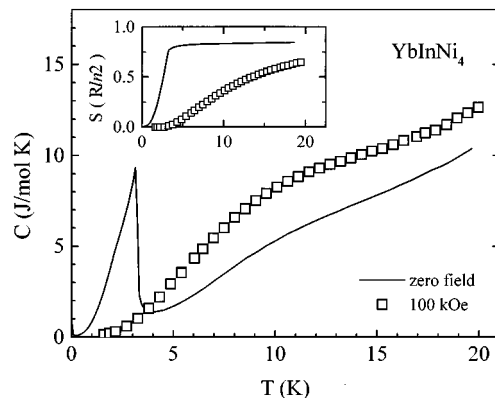


FIG. 3. Specific heat as a function of temperature for YbInNi_4 for $H=0$ (solid line) and $H=100$ kOe (squares). The corresponding magnetic entropy (in units of $R \ln 2$) is shown in the inset. See text for details.

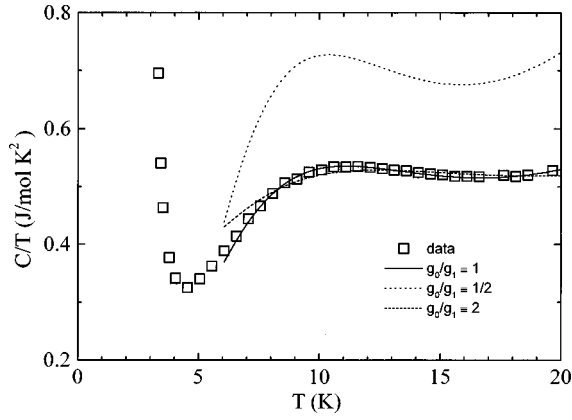


FIG. 4. Specific heat divided by temperature as a function of temperature for YbInNi₄. The squares represent the data, and the lines represent fits to the data assuming different crystal-field level degeneracies. See text for details.

nated both by the sharp magnetic ordering peak at 3 K as well as by a broad Schottky-like anomaly centered near 10–15 K. The data above 8 K are well described by a standard model that consists of an electronic contribution, a lattice contribution, and a Schottky contribution to C_p that is given by

$$C = \gamma T + \beta T^3 + R \left(\frac{\delta}{T} \right) \frac{g_0}{g_1} \frac{\exp(\delta/T)}{[1 + (g_0/g_1)\exp(\delta/T)]^2}, \quad (1)$$

with a Sommerfeld coefficient of $\gamma = 150$ mJ/mole K², a T^3 phonon contribution with $\Theta_D = 272$ K, and a Schottky contribution with an energy splitting of $\delta = 32$ K. By subtracting these terms from the total measured C_p data it is possible to integrate the remaining specific heat to determine the magnetic entropy associated with the ferromagnetic transition. The observed entropy is very close to $R \ln 2$ (see inset to Fig. 3), indicating that the ferromagnetic order arises from a ground-state doublet. The specific heat rises below 200 mK, presumably due to a nuclear Schottky contribution stemming from the influence of the internal field on nuclear hyperfine energy levels. The application of a 100-kOe magnetic field acts to smear the ferromagnetic transition considerably (open squares in Fig. 3), while the $R \ln 2$ entropy is still recovered by 20 K. These in-field results are fully consistent with conventional ferromagnetic order.

The Schottky contribution to the specific heat is analyzed in greater detail in Fig. 4 where the data is plotted as C/T vs T . The near temperature-independence of C/T above 10 K is a clear indication that a low-lying Schottky anomaly is present in YbInNi₄. The eightfold degenerate ground state of Yb is split into two doublets and a quartet in the presence of a cubic crystal field.³² As such, the ratio of the degeneracies of the ground state g_0 to the first excited state g_1 can be $g_0/g_1 = 1/2$, 1, or 2 for a doublet-quartet, doublet-doublet, or quartet-doublet configuration, respectively. These three level schemes can be tested by fitting the data in Fig. 4 with Eq. (1), and the resulting fits are shown in the figure. The fits clearly reveal that a doublet-doublet configuration with an energy splitting of $\delta = 32$ K is most consistent with the data; this level splitting is also consistent with there being a broad feature in the resistivity data at roughly 20 K.

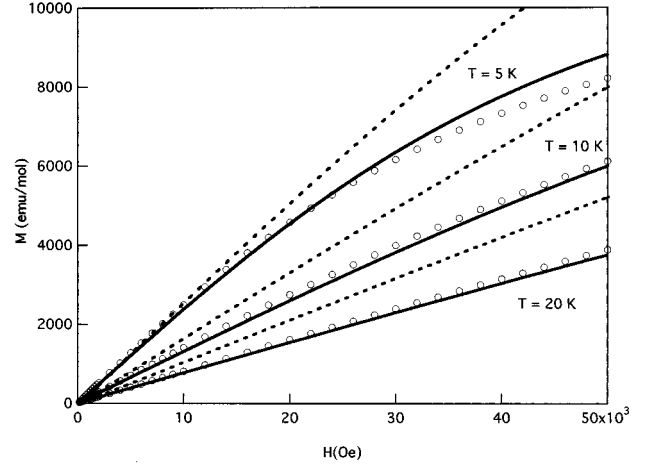


FIG. 5. Isothermal magnetization as a function of applied field at various fixed temperatures for YbInNi_{3.25}Cu_{0.75}. The circles are the experimental data and the solid lines represent a simultaneous fit to the 5, 10, and 20 K data. This fit corresponds to a ground-state doublet, an excited doublet at 64 K and a quartet at 122 K above the ground state [$x = 0.53$, $W = 0.48$ meV (Ref. 32)]. See text for details. For comparison, the dashed lines show the magnetization that would be expected for the crystal-field scheme [$x = 0.38$, $W = -0.17$ meV (Ref. 32)] determined by Severing *et al.* for YbInNi₄ (Ref. 16).

Further insight into the crystal-field state of YbInNi₄ may be gained by more carefully examining the magnetization as a function of field at fixed temperature. Unfortunately, the presence of magnetic order complicates this analysis. Therefore, we have doped YbInNi₄ with sufficient Cu (approximate composition YbInNi_{3.25}Cu_{0.75}) to suppress long-range magnetic order. Despite the addition of this chemical disorder, it is reasonable to assume that the crystal-field state of Yb is, at least qualitatively, unchanged. The magnetization as a function of field for this sample is shown in Fig. 5. The magnetization is fit simultaneously using the 5, 10, and 20 K data. The crystal-field scheme that best fits these data is a ground-state doublet with an excited doublet 64 K above the ground state and with the quartet an additional 58 K above the excited doublet ($x = 0.53$, $W = 0.48$ meV in the notation of Lea, Leask, and Wolf³¹). Although the magnetization-derived crystal-field scheme has a somewhat larger splitting than that inferred from specific heat and resistivity, the relative level spacing and degeneracies are retained.

In Fig. 6 we show the magnetization of YbInNi₄ at 4 K as a function of magnetic field up to 600 kOe. The magnetization reaches a value of $3.25\mu_B/\text{Yb}$, close to the expected $g \cdot J$ value of $4\mu_B$ for the full multiplet of Yb ($g = 8/7$, $J = 7/2$), and no metamagnetic transitions are observed. Thus, despite the significant impact of crystal fields on the low-temperature, low-field properties of YbInNi₄, in sufficiently large magnetic fields, the behavior of the full Yb multiplet is recovered.

YbInNi₄ displays an appreciable negative magnetoresistance for temperatures much greater than $T_c = 3$ K. This can be seen clearly in Figs. 7 and 8. In Fig. 7 we show the resistance as a function of temperature in zero-applied field and in an applied field of 180 kOe. The magnetic field was applied in a direction perpendicular to the measurement cur-

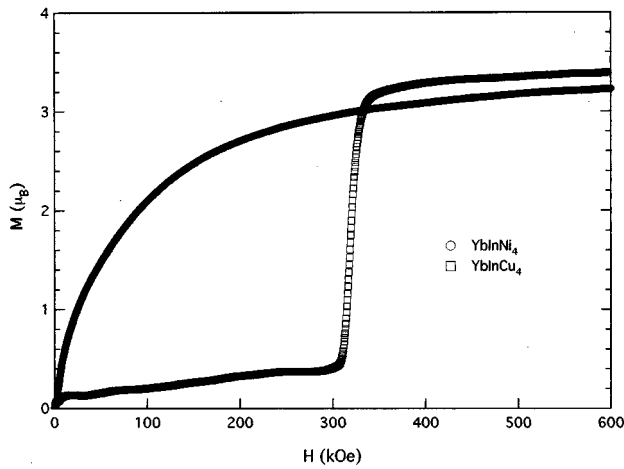


FIG. 6. Isothermal magnetization of YbInNi_4 at 4 K, measured using a 600-kOe pulsed magnet. For comparison data for YbInCu_4 , which undergoes a field-induced, first-order valence transition (Ref. 6), are also shown.

rent. For $T \leq 100$ K, the applied field reduces the sample resistance, and the resulting resistance as a function of temperature is relatively featureless and typical of a metal. In Fig. 8(a) we show the transverse magnetoresistance $\{\Delta R \equiv [R(B) - R(B=0)]/R(B=0)\}$ as a function of magnetic field at various fixed temperatures. Negative magnetoresistances as large as 50% are observed. In the inset of Fig. 8(b), we show the magnetoresistance as a function of magnetic field for $T \leq T_c$ on an expanded scale. The saturated magnetoresistance decreases with decreasing temperature, suggesting that domain effects are dominant in the ferromagnetically ordered state.

In Fig. 8(b) we replot the magnetoresistance data for $T > 8$ K as a function of magnetic field divided by temperature (H/T). Remarkably, the data collapse onto a single curve. For $T < 8$ K, this scaling breaks down. It is interesting to note that this is the temperature at which ferromagnetic correlations begin to dominate the magnetic susceptibility— $\chi \cdot T$

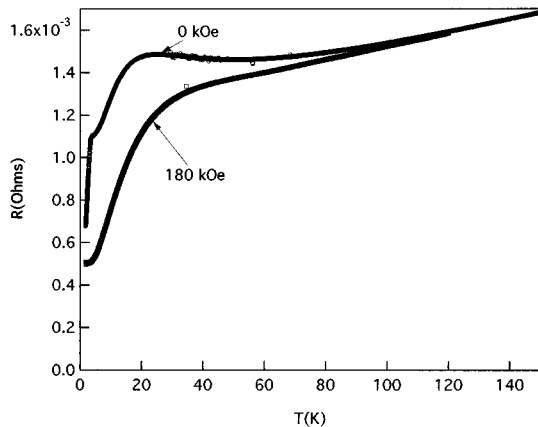
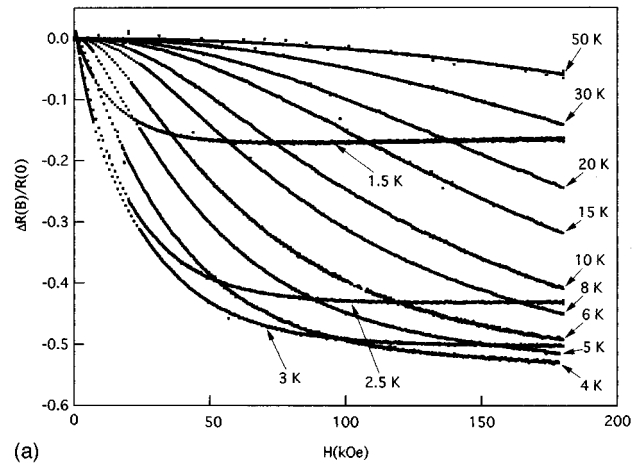
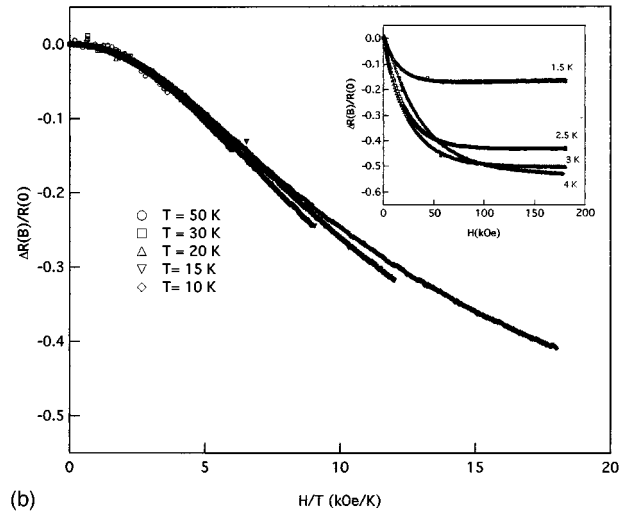


FIG. 7. Resistance as a function of temperature for YbInNi_4 in magnetic fields of 0 and 180 kOe. The magnetic field was applied perpendicular to the applied current. Note the appreciable magnetoresistance at temperatures as high as 120 K.



(a)



(b)

FIG. 8. (a) Transverse magnetoresistance $[R(B) - R(B=0)]/R(B=0)$ as a function of applied field at various fixed temperatures for YbInNi_4 . (b) The data of Fig. 8(a) plotted as a function of H/T . For $T \geq 8$ K, the data collapse onto a single curve. The data for $T \leq T_c$ are shown in the inset. Note that the magnitude of the magnetoresistance at high field decreases with decreasing temperature.

passes through a minimum at 8 K (not shown). On the other hand, Kohler's rule is poorly obeyed: the data plotted as a function of $B/\rho(B=0, T)$ (not shown) are qualitatively similar to that of Fig. 8(a), indicating that the scattering rate is not independent of magnetic field (a necessary condition for the applicability of Kohler's rule).³³

Although magnetoresistance that is proportional to H/T is not atypical of f -electron materials, the range of temperature over which this scaling is observed is rather large. Two common mechanisms give rise to such behavior. Scattering from independent Kondo impurities produces magnetoresistance that is a universal function of B/B^* , where B^* is a characteristic field given by $B^*(T) = k_B(T_K + T)/(g\mu)$.³⁴ However, attempts to improve the scaling of our data by replotting as a function of $T + T_K$ give rise to values of T_K that do not vary monotonically with T —i.e., assuming $T_K = T_K(T)$ (Ref. 35)—and do not substantially improve the collapse of our data. On the other hand, Beal-Monod and Weiner have shown that $\Delta R \propto M^2$ should result from the suppression of normal spin-flip scattering due to the polarization of local

moments by the applied field.³⁶ In fact, our data, for small values of H/T , are well described by $\Delta R = -a(H/T)^2$, with a a positive constant. At large values of H/T , where $M = \chi H$ becomes a bad approximation due to saturation effects, our data deviate from this behavior. Unfortunately, we have not been able to measure isothermal magnetization in sufficiently high magnetic fields to test the extent to which $\Delta R \propto M^2$ experimentally.

IV. DISCUSSION

From the data presented in Sec. III, YbInNi₄ appears to be a rather conventional f -electron material in which crystal-field effects are dominant and ferromagnetism arises at low temperature out of a doublet ground state. These experimental observations are somewhat troubling for several reasons. In 1990 Severing *et al.*¹⁶ performed inelastic neutron-scattering measurements on YbInCu₄ and YbInNi₄ and found evidence for a quartet ground state in both of these materials. This conclusion appears to be straightforward because direct doublet-doublet transitions within Yb's crystal-field multiplet in a cubic crystal field are forbidden by symmetry. Thus, the observation of two distinct crystal-field excitations—as observed by Severing *et al.* for both YbInCu₄ and YbInNi₄—is a clear signature of a quartet ground state. Intensity analysis of the neutron data is also consistent with a ground-state quartet, and the magnetization inferred from the neutron data is in good agreement with that measured by bulk susceptibility.¹⁶ Furthermore, in the case of YbInCu₄, our own specific-heat data³⁷ show that approximately $R \ln 6$ of entropy is liberated at the first-order valence transition, strongly suggestive of a greater-than-doublet ground-state degeneracy for YbInCu₄. It is difficult to understand how relatively similar ligand ions can produce such a large change in the crystal electric field; however, YbInNi₄ is a substantially better metal than YbInCu₄, as deduced from Hall-effect measurements, and the increased conduction electron density may provide sufficiently enhanced hybridization to modify one's point-charge expectations. Thermodynamic³⁸ and electron paramagnetic resonance³⁹ experiments on YbInNi_{4-x}Cu_x are currently underway to clarify these issues. However, if one calculates the magnetization as a function of field at fixed temperature that would be expected from the neutron-inferred crystal-field scheme for YbInNi₄ (see Fig. 5), the result is clearly inferior to the crystal-field scheme discussed above. It is perhaps possible that these differences could arise due to a disorder effect—Severing *et al.* studied polycrystalline material whereas all of our results were obtained with single-crystal samples; however, such a conclusion seems unlikely. In any event, inelastic neutron-scattering experiments on single crystals of YbInNi₄ would appear to be warranted.

The appearance of ferromagnetism in YbInNi₄ is also somewhat unexpected. Buschow *et al.*⁴⁰ have argued that, at least in pseudobinary compounds, Yb-Ni compounds favor a higher-valence state than do Yb-Cu compounds. It, therefore, may not be surprising that Kondo effects (which act to reduce the effective Yb moment) are dominant in YbInCu₄, to the extent that a first-order valence change is observed,³⁻¹⁰ whereas local moment behavior is dominant in YbInNi₄. In fact, two of the three other compounds in which Yb orders

ferromagnetically (YbNiSn and Yb₂Ni₁₇) are compounds in which Ni is present. However, Kondo physics plays a dominant role in YbNiSn,¹⁹⁻²¹ and the ferromagnetic ordering of the Ni sublattices at higher temperature appears to influence the ordering of Yb in Yb₂Ni₁₇.^{22,23}

If one applies a Friedel-type analysis⁴¹ to the YbXM₄ compounds that are known to order magnetically (YbInNi₄, YbAuCu₄, and YbPdCu₄), the results are ambiguous. $F(k_F a)$, where $F(x) = (x \cos x - \sin x)/x^4$, k_F is the Fermi momentum and a is the spacing between magnetic ions, changes sign between YbInNi₄ and YbAuCu₄ (which orders antiferromagnetically¹⁴), assuming a single-band picture in which the Hall constant $R_H = 1/ne$,⁴² and taking a as the Yb-Yb distance. However, this simple analysis would predict antiferromagnetic order for YbInNi₄ and ferromagnetic order for YbAuCu₄. Because of sample purity problems, it has not been possible to obtain a good estimate of the Hall coefficient of YbPdCu₄ (which appears to order ferromagnetically¹⁴ rather than antiferromagnetically, as previously reported¹¹). It is possible that a more careful analysis, including greater than nearest-neighbor interactions and a more realistic treatment of the electronic band structure, could explain the origin of ferromagnetism in YbInNi₄.

Finally, it is interesting to note that despite their drastically different low-temperature, low-field behavior, YbInNi₄ and YbInCu₄ are quite similar in high magnetic fields. Both materials have nearly identical magnetizations above 400 kOe (see Fig. 6)—the 5% difference at high field may well be within experimental uncertainty: the absolute calibration for YbInCu₄ is rather difficult given the small magnitude of the signal at low field (where comparison to magnetometer data is possible) and the enormous change in signal size at the valence transition. Apparently, the large Zeeman energy supplied by the magnetic field overwhelms the low-energy-scale effects of the Kondo interaction (in the case of YbInCu₄) and the effects of crystal-electric fields (in the case of YbInNi₄) to the extent that the magnetization of the full Yb multiplet is manifest at high field.

V. CONCLUSION

We have shown that ferromagnetism arises in YbInNi₄ at low temperature out of a crystal-field-dominated ground state. This ground state possesses both enhanced electronic specific heat and an appreciable and rather universal negative magnetoresistance. Further work is needed to resolve the differences between the crystal-field scheme inferred from our thermodynamic measurements and that inferred from earlier neutron-scattering results.¹⁶ The detailed nature of the ferromagnetism in YbInNi₄ and the associated magnetoresistance also merit further study.

ACKNOWLEDGMENTS

A.H.L. is thankful to J. Detwiler for helping with the experiments. Work at LANL is performed under the auspices of the U.S. Dept. of Energy. The NHMFL is supported by the NSF and the state of Florida through Cooperative Agreement No. DMR-9527035. Some of us also gratefully acknowledge support from the NSF through Grant No. DMR-9501529 (J.L.S., C.L.B., C.D.I., M.E.T., and Z.F.) and Grant No. DMR-9705155 (S.B.O.).

- ¹Z. Fisk and M. B. Maple, *J. Alloys Compd.* **183**, 303 (1992).
- ²E. Bauer, *Adv. Phys.* **40**, 417 (1991).
- ³J. M. Lawrence, G. H. Kwei, J. L. Sarrao, Z. Fisk, D. Mandrus, and J. D. Thompson, *Phys. Rev. B* **54**, 6011 (1996).
- ⁴J. L. Sarrao, C. D. Immer, C. L. Benton, Z. Fisk, J. M. Lawrence, D. Mandrus, and J. D. Thompson, *Phys. Rev. B* **54**, 12 207 (1996).
- ⁵A. L. Cornelius, J. M. Lawrence, J. L. Sarrao, Z. Fisk, M. F. Hundley, G. H. Kwei, J. D. Thompson, C. H. Booth, and F. Bridges, *Phys. Rev. B* **56**, 7993 (1997).
- ⁶C. D. Immer, J. L. Sarrao, Z. Fisk, A. Lacerda, C. Mielke, and J. D. Thompson, *Phys. Rev. B* **56**, 71 (1997).
- ⁷J. M. Lawrence, S. M. Shapiro, J. L. Sarrao, and Z. Fisk, *Phys. Rev. B* **55**, 14 467 (1997).
- ⁸B. Kindler, D. Finsterbusch, R. Graf, F. Ritter, W. Assmus, and B. Luthi, *Phys. Rev. B* **50**, 704 (1994).
- ⁹J. M. de Teresa, Z. Arnold, A. del Moral, M. R. Ibarra, J. Kamard, D. T. Adroja, and B. Rainford, *Solid State Commun.* **99**, 911 (1996).
- ¹⁰I. Felner and I. Nowik, *Phys. Rev. B* **33**, 617 (1986); I. Felner *et al.*, *ibid.* **35**, 6956 (1987); I. Nowik *et al.*, *ibid.* **37**, 5633 (1988).
- ¹¹C. Rossel, K. N. Yang, M. B. Maple, Z. Fisk, E. Zirngiebl, and J. D. Thompson, *Phys. Rev. B* **35**, 1914 (1987).
- ¹²T. Graf *et al.*, *Phys. Rev. B* **52**, 3099 (1995); T. Graf *et al.*, *ibid.* **51**, 15 053 (1995).
- ¹³A. Severing, A. P. Murani, J. D. Thompson, Z. Fisk, and C.-K. Loong, *Phys. Rev. B* **41**, 1739 (1990).
- ¹⁴E. Bauer, P. Fischer, F. Marabelli, M. Ellerby, K. A. McEwen, B. Roessli, and M. T. Fernandes-Dias, *Physica B* **234-236**, 676 (1997).
- ¹⁵E. Bauer, E. Gratz, R. Hauser, Le Tuan, A. Galatanu, A. Kottar, H. Michor, W. Perthold, G. Hilscher, T. Kagayama, G. Oomi, N. Ichimiya, and S. Endo, *Phys. Rev. B* **50**, 9300 (1994).
- ¹⁶A. Severing, E. Gratz, B. D. Rainford, and K. Yoshimura, *Physica B* **163**, 409 (1990).
- ¹⁷A. E. Dwight, *J. Less-Common Met.* **43**, 117 (1975).
- ¹⁸I. Felner, *Solid State Commun.* **21**, 267 (1977).
- ¹⁹P. Bonville, P. Bellot, J. A. Hodges, P. Imbert, G. Jehanno, G. Le Bras, J. Hammann, L. Lelyekian, G. Chevrier, P. Thuery, L. D'Onofrio, A. Hamzic, and A. Barthelemy, *Physica B* **182**, 105 (1992).
- ²⁰M. Kasaya, T. Tani, F. Iga, and T. Kasuya, *J. Magn. Magn. Mater.* **76&77**, 278 (1988); M. Kasaya, T. Tani, K. Kawate, T. Mizushima, Y. Isikawa, and K. Sato, *J. Phys. Soc. Jpn.* **60**, 3145 (1990).
- ²¹A. L. Cornelius, J. S. Schilling, D. Mandrus, and J. D. Thompson, *Phys. Rev. B* **52**, 15 699 (1995).
- ²²P. Bonville, J. Hammann, J. A. Hodges, P. Imbert, and G. Jehanno, *J. Magn. Magn. Mater.* **151**, 115 (1995).
- ²³P. D. Carfagna and W. E. Wallace, *J. Appl. Phys.* **39**, 5259 (1968).
- ²⁴B. Politt, Ph.D. thesis, Universitat Koln, 1987.
- ²⁵G. Heinrich, J. P. Kappler, and A. Meyer, *Phys. Lett.* **74A**, 121 (1979).
- ²⁶A. P. Ramirez, B. Batlogg, and Z. Fisk, *Phys. Rev. B* **34**, 1795 (1986).
- ²⁷J. D. Thompson, Z. Fisk, and J. O. Willis, in *Proceedings of the 17th International Conference on Low Temperature Physics (LT17)*, edited by U. Eckern, A. Schmid, W. Weber, and H. Wuhl (North-Holland, Amsterdam, 1984), p. 323.
- ²⁸U. Walter, Z. Fisk, and E. Holland-Moritz, *J. Magn. Magn. Mater.* **47&48**, 159 (1985).
- ²⁹R. Bachmann, F. J. DiSalvo, T. H. Geballe, R. L. Greene, R. E. Howard, C. N. King, H. C. Kirsch, K. N. Lee, R. E. Schwall, H.-U. Thomas, and R. B. Zubeck, *Rev. Sci. Instrum.* **43**, 205 (1972).
- ³⁰B. Cornut and B. Coqblin, *Phys. Rev. B* **5**, 4541 (1972).
- ³¹S. Doniach, in *Valence Instabilities and Related Narrow Band Phenomena*, edited by R. D. Parks (Plenum, New York, 1977), p. 169.
- ³²K. R. Lea, M. J. M. Leask, and W. P. Wolf, *J. Phys. Chem. Solids* **23**, 1381 (1962).
- ³³A. B. Pippard, *Magnetoresistance in Metals* (Cambridge University Press, Cambridge, 1989).
- ³⁴P. Schlottmann, *Z. Phys. B* **51**, 223 (1983).
- ³⁵B. Batlogg, D. J. Bishop, E. Bucher, B. Golding, A. P. Ramirez, Z. Fisk, and J. L. Smith, *J. Magn. Magn. Mater.* **63&64**, 441 (1987).
- ³⁶M. T. Beal-Monod and R. A. Weiner, *Phys. Rev.* **170**, 552 (1968).
- ³⁷A. P. Ramirez *et al.* (unpublished).
- ³⁸R. Modler *et al.* (unpublished).
- ³⁹C. Rettori *et al.* (unpublished).
- ⁴⁰K. H. J. Buschow, M. Brouha, H. J. van Daal, and A. R. Miedema, in *Valence Instabilities and Related Narrow Band Phenomena* (Ref. 31), p. 125.
- ⁴¹C. Kittel, *Quantum Theory of Solids* (Wiley, New York, 1987).
- ⁴²E. Figueroa *et al.* (unpublished).